Biomedical Research 2019; 30 (4) *ISSN 0970-938X*
www.biomedres.info

Independent behaviors of myostatin and E3 ubiquitin ligases in atrophied fast and slow skeletal muscles.

Kihyuk Lee[1,2], Takahiro Maekawa[3], Karina Kouzaki[1], Hongsun Song[4*], Koichi Nakazato[1]

[1]Department of Exercise Physiology, Nippon Sport Science University, Tokyo, Japan

[2]Center for Sport Science in Jeju, Jeju Special Self-Governing Provincial Sports Council, Jeju, Korea

[3]Department of Rehabilitation for the Movement Functions, Research Institute, National Rehabilitation Center for Persons with Disabilities, Saitama, Japan

[4]Department of Sports Science, Korea Institute of Sport Science, Seoul, Korea

Abstract

In skeletal muscle, the expression of myostatin and activation of muscle-specific E3 ubiquitin ligases play roles in protein degradation and atrophy. Although fiber-type dependency of myostatin expression has been reported, it is unclear whether the relationship between myostatin expression and activation of muscle-specific E3 ubiquitin ligases shows a similar tendency The objective of this study was to determine whether expressions of myostatin and muscle-specific E3 ubiquitin ligases differ, depending on fiber type in muscle atrophy induced by nerve crush injury (NCI) to the rat sciatic nerve. Soleus (rich in slow-twitch fibers) and plantaris (rich in fast-twitch fibers) muscles were analysed by Western blotting and immunohistochemistry. The wet weight of the plantaris muscle decreased gradually, reaching a minimum on 14th day after NCI, while the wet weight of the soleus muscle was lowest after 7th day. The cross sectional area (CSA) of type II muscle significantly reduced both soleus and plantaris muscle, but the type I muscle did not significantly decrease in plantaris muscle. The expression of muscle RING finger protein 1 (MuRF1) and muscle atrophy F-box (MAFbx)/atrogin-1, muscle-specific E3 ubiquitin ligases, were significantly higher in both soleus and plantaris muscles on day 3 after NCI compared to the untreated control group. A significantly increased level of myostatin was seen in plantaris muscle only on day 14 after NCI. We conclude that myostatin expression in NCI-induced muscle atrophy plays a role in only fast-twitch muscle atrophy. On the other hand, expressions of the MuRF1 and MAFbx are independent from fiber type.

Keywords: Nerve crush injury, Muscle fiber type, Myostatin, MuRF1, MAFbx/atrogin-1.

Accepted on January 12, 2019

Introduction

Skeletal muscle atrophy is induced by disuse, aging, nerve damage, and diseases [1-3]. Several researchers have studied the mechanisms of skeletal muscle atrophy [4-6]. In general, mechanistic experiments of skeletal muscle atrophy have used immobilization and denervation models [7]. In addition, the fashion of skeletal muscle atrophy seems to be dependent on muscle fiber type [8-10].

Although the mechanism of fiber-specific muscle atrophy is unclear, it has been reported that immobilization induces skeletal muscle atrophy due to disuse and denervation-induced atrophy and mainly decreasing muscle fibers which are slow-twitch fibers [11,12]. On the other hand, the atrophy of fast-twitch fibers is attributed to cancer cachexia and aging [13,14]. The molecular mechanism and phenomenon about muscle atrophy using inactivity and denervation model have been reported [15,16]. However, at the molecular level, it is not fully elucidated whether fiber-specific atrophy can be attributed to different signaling pathways. Moreover, it is not clear whether nerve damage-induced atrophy proceeds faster rate in slow-twitch than in fast-twitch fibers.

The ubiquitin-proteasome system (UPS) is reportedly the major cause of skeletal muscle atrophy [17,18]. This system induces protein degradation by up-regulating two muscle-specific ubiquitin ligases, muscle atrophy F-box (MAFbx, also called atrogin-1) and muscle RING finger 1 (MuRF1) [19-21]. Myostatin, which belongs to the transforming growth factor-beta superfamily, is a negative regulator of muscle mass [22]. Protein degradation by myostatin is dependent on forkhead box 1 (FoxO1) activity [23]. Furthermore, regulation of FoxO proteins induces muscle protein degradation *via* the UPS [24]. Although one group reported that myostatin expression induced protein degradation *via* up-regulation of MAFbx and

FoxO1 [25], it is not clear whether the myostatin-FoxOs-UPS axis plays a role in compliance with muscle fiber type.

Nerve damage can cause skeletal muscle atrophy [26]. In particular, denervation (i.e., cutting of the nerve trunk) is used to investigate the mechanism of muscle atrophy [27]. Although many studies have reported that denervation triggers the expression of atrophy-related factors (i.e., MAFbx, MuRF1, FoxO1, FoxO3a, and myostatin) [28-30], complete cutting of a nerve (neurotmesis) is a clinically uncommon form of nerve damage [31]. Nerve crush injury (NCI) is the usual form of nerve injury, and it can involve neuropraxia (myelin damage) or axonotmesis (partial axonal damage) according to Seddon's classifications [31]. However, the detailed molecular mechanism of NCI-induced atrophy has not been elucidated. Lin et al. [26] reported that NCI-induced muscle atrophy involved myostatin expression in gastrocnemius muscle, which is a mixture of fast and slow fibers. It is unclear whether myostatin plays a role in NCI-induced muscle atrophy depending on muscle fiber type. Moreover, the relationship between myostatin expression and UPS activation has not been examined in NCI-induced muscle atrophy, especially with regard to fiber type dependency.

The objective of the present study was to examine whether myostatin expression and UPS activation were dependent on muscle fiber type in NCI-induced muscle atrophy.

Materials and Methods

Animal care

Male Wistar rats (age, 6 weeks; n=32) were randomly assigned to the following two groups: sham operation group (Con; n=8) and nerve crush injury group (NCI, n=24). They were familiarized for 2 weeks and then subjected to NCI. Furthermore, NCI groups were divided into three groups for analysis of time course (3 days, 7 days, and 14 days group). The rats were individually housed in ventilated cage (IVC) systems (Tecniplast, Milan, Italy) maintained at 22-24°C with a 12 hour light/dark cycle. Rats were provided water and food *ad libitum*. On day 3, day 7 and day 14 after NCI, 8 rats in each group were killed. Sham operation group was killed after NCI. This study was approved by the Ethical Committee for Animal Experiments at the Nippon Sport Science University.

Surgical procedures of nerve crush injury

NCI was conducted according to the previous reported study. Briefly, the right hind limbs of all the rats were shaved, and then each rat was anesthetized with isoflurane (aspiration rate, 450 ml/min; concentration, 2.0%). The right sciatic nerve was exposed through an incision of the skin above the right hind leg. The exposed sciatic nerve was crushed using a forcep clamping for 30 seconds. Left sciatic nerve was left intact. Only incision of the skin was made in the sham-operated control group. After NCI, the incision of skin above right hind leg was stitched and rats were returned to their cages. On day 3, 7 and 14 after surgery, each group was killed. Because we speculated that the relationship between myostatin and the UPS was dependent on muscle fiber type, analysed both soleus (abundant in slow fibers) and plantaris (abundant in fast fibers) muscles in the present study. Specimens were weighed, and immediately frozen in liquid N_2. Frozen materials were stored at -80°C until analysis.

Western blotting

The soleus and plantaris muscles of each group (n=6) were macerated in liquid N_2 and homogenized using a RIPA buffer (Pierce, Rockford, USA). The homogenate was centrifuged at 16,000 Xg for 15 minutes at 4°C and supernatant was obtained. Protein concentrations were determined using a protein concentration determination kit (Protein Assay II; Bio-Rad, Richmond, VA). A 30 μg total protein extracts from each sample were mixed with sample buffer, boiled, loaded on the same SDS-polyacrylamide gel (12.5%). The samples were electrophoretically separated and separated proteins were then transferred onto nitrocellulose membranes (GE healthcare, Whatman, Germany). The membranes were blocked for 1 h with tris-buffered saline (TBS) containing 1% triton X and 5% skimmed milk and then incubated overnight at 4°C with the following primary antibodies (dilution, 1:1000): anti-GDF8 (sc-6884; Santacruz Biothechnology), anti-MuRF1 (sc-32920; Santacruz Biothechnology): anti-MAFbx/atrogin-1 (sc-33782; Santacruz Biothechnology). The membranes were then washed three times and incubated with the secondary antibody at room temperature. Horseradish peroxidase (HRP)-conjugated goat anti-mouse immunoglobulin G (IgG) or anti-rabbit IgG (dilution, 1:10,000) was used as the secondary antibody. Chemiluminescent reagents were used for detecting the secondary antibody (Super Signal West Dura; Pierce Protein Research Products, Rockford, IL). Chemiluminescent signals were detected using a chemiluminescence detector (AE9100N; ATTO) and quantified using a personal computer with image analysis software (CS Analyzer; ATTO). The band densities were showed relative to those obtained for the control. All targets proteins were normalized by total protein stained with Ponceau S.

Immunohistochemistry

The soleus and plantaris muscles of each group (n=2) were embedded in OCT compound using isopentane and frozen in liquid N_2. The frozen samples stored at -80°C. Cross-sections (10 μm thick) were cut with a cryostat at -20°C and mounted on glass slides. After glass slides were then washed three times for 10 minutes, the sections were blocked with 0.1 M PBS containing 1% bovine serum albumin and 0.01% Triton X-100 for 1hours to block any nonspecific reaction. The sections were then incubated with the primary antibodies including anti-type I myosin (1:300; M-8421, SIGMA) and anti-dystrophin (1:500; sc-15376, Santacruz Biothechnology) diluted with 0.1 M PBS containing 1% bovine serum albumin and 0.01% Triton X-100 overnight at 4°C. The secondary antibodies were used Alexa Fluor 488 goat anti-rabbit green IgG (A-11008; Molecular Probes) and Alexa Fluor 568 goat anti-mouse red IgG

(A-11019; Invitrogen) for 2 hours. After the secondary antibodies incubation, the sections were washed three times 0.1 M PBS for 10 minutes and were cover-slipped with mounting medium with DAPI (Vectashield, Vector Laboratories). The sections were viewed with florescence microscope (Olympus model BX 60; Olympus, Japan), and the images were captured with a digital camera (Olympus model DP 70; Olympus, Japan), and analysed using Olympus DP 70 controller software. Cross-sectional area (CSA) of the plantaris and soleus muscles fibers (approximately 100 fibers per muscle) was analysed using Image J analysis software (National Institutes of Health, Bethesda, MD, USA).

Statistical analysis

All values are expressed as means ± standard error of the mean (SE). One-way analysis of variance (ANOVA) followed by Fisher's least significant difference (LSD) was used to compare the body mass, wet weight of soleus and plantaris muscles, protein levels, and CSA using SPSS 22 (IBM, Chicago, IL, USA). The significance level was set at $P<0.05$.

Results

Wet weights and CSA of soleus and plantaris muscles following NCI

Following NCI, no significant differences in the body weights were observed as compared to controls (Table 1). However, the wet weights of both the right soleus and right plantaris muscles significantly decreased with time, reaching minimums on day 7 (Con *vs.* day 7 of NCI; soleus: 68%, $p<0.01$) and day 14 (Con *vs.* day 14 of NCI; plantaris: 59%, $p<0.01$), respectively (Table 1). As with the reduction of wet weight of soleus and plantaris muscles, CSAs of muscle-fiber types I and II in soleus muscle of 7th and 14th day (Figures 1A and 1B) were significantly smaller than that of the control group ($p<0.05$) ($p<0.01$). CSA of muscle-fiber type II in plantaris muscle of 7th and 14th day (Figure 2B) were significantly smaller than that of the control group ($p<0.01$). There was no significant dierence in CSA of muscle-fiber type I in plantaris muscle.

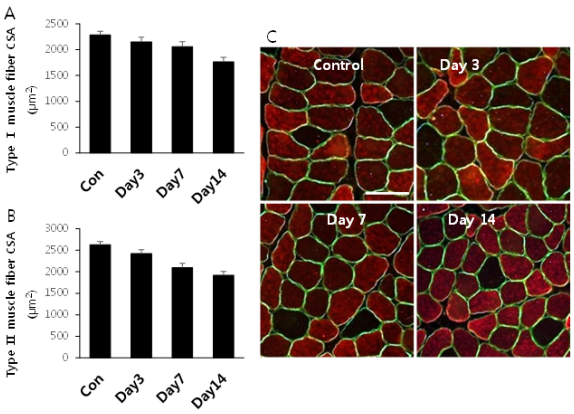

Figure 1. *CSA of soleus muscle after NCI.*

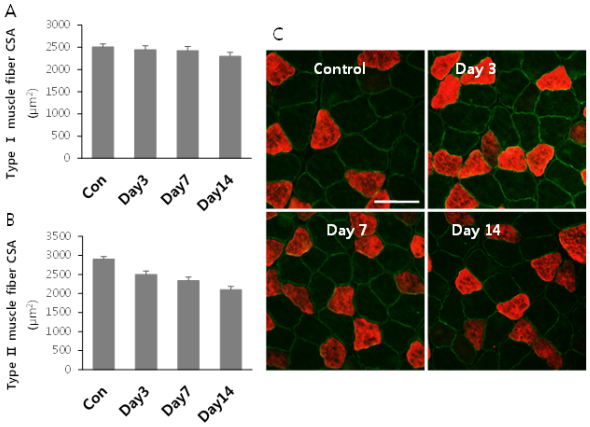

Figure 2. *CSA of plantaris muscle after NCI.*

Effects of NCI on MuRF1 and MAFbx/atrogin-1 expression in soleus and plantaris muscles

The expression of MuRF1 and MAFbx/atrogin-1 was measured using Western blot analysis. These were significantly higher than that of the control group on day 3 after NCI in both soleus and plantaris muscles ($p<0.01$; $p<0.01$; Figures 3 and 4).

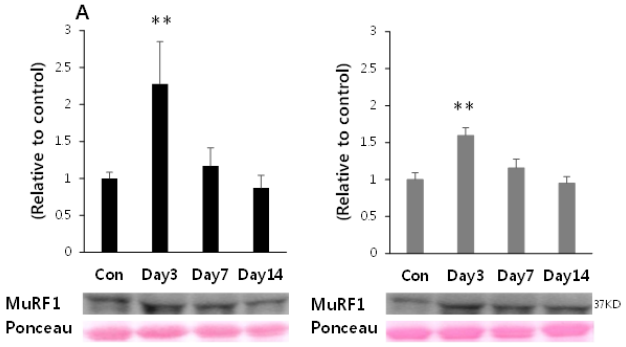

Figure 3. *The time course change in expression of MuRF1.*

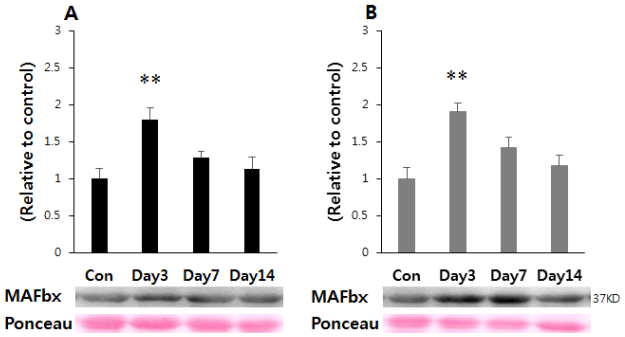

Figure 4. *The time course change in expression of MAFbx/atrogin.*

Muscle fiber type dependency of myostatin expression in NCI

In order to confirm muscle fiber type dependency of myostatin expression, the expression of myostatin was measured using western blot analysis. Significantly increased expression of

myostatin was only observed in plantaris muscle 14 days after NCI ($p<0.01$; Figure 5). This increase was not evident in soleus muscle.

Table 1. *Body weight and wet weight of soleus and plantaris muscle after NCI. Values are expressed as mean ± SE.* $^{**}p<0.01$*, significantly different from Con.*

	Con	Day 3	Day 7	Day 14
BW (g)	283.12 ± 9.96	266.10 ± 17.16	280.38 ± 22.02	284.98 ±7.98
Soleus/BW (mg/g)	3.98 ± 0.22	3.49 ± 0.37**	2.71 ± 0.39**	2.74 ± 0.67
Soleus (mg)	1124.83 ± 31.19	929.83 ± 124.00**	764.00 ± 155.20**	788.33 ± 206.30
Plantaris/BW (mg/g)	9.75 ± 0.36	7.85 ± 0.53**	6.87 ± 0.50**	5.82 ± 0.60**
Plantaris (mg)	2760.50 ± 116.28	2094.83 ± 271.30**	1929.50 ± 242.93**	1661.33 ± 205.53**

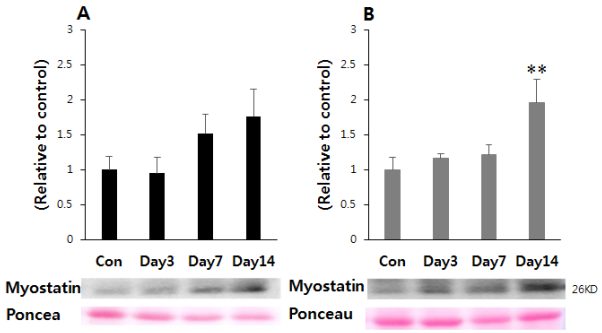

Figure 5. *The time course change in expression of myostatin.*

Discussion

The results of the present study showed that NCI similarly reduced the wet weight of soleus and plantaris muscle. This is not consistent with other studies reporting that the time course of muscle atrophy differs according to the muscle fiber type [32,33]. Previous studies have reported that slow-twitch muscle fibers atrophied faster, and showed more atrophy than fast-twitch fibers in the immobilization and denervation models [11,12,34].

In the current study, we found that the rate of muscle mass reduction was similar between soleus and plantaris muscle, but the peak reduction was late in plantaris than in soleus muscle. In general, disuse-related skeletal muscle atrophy, as occurs following denervation and immobilization, occurs primarily in slow-twitch (oxidative-related) fibers. In contrast, nutrient-related atrophy-such as cancer/aging cachexia, sepsis, and diabetes-is more highly directed to the loss of fast-twitch (glycolytic-related) fibers [6,9,10]. We confirmed that body weight was maintained after the experimental period. In addition, CSA of type II muscle significantly reduced both soleus and plantaris muscle, but the type I muscle did not significantly decrease in plantaris muscle. Thus, disuse-related muscle atrophy appears to occur in the NCI model, similar to the denervation model [7,33]. Because, only neuroplaxia and axonotomesis occur in NCI, we did not observe more muscle reduction in soleus than in plantaris muscle, as occurs in the denervation (neurotomesis) model [7,33].

Many studies have reported that the up-regulation of MuRF1 and MAFbx induce muscle protein degradation and appears within 3 days in immobilization and denervation models of atrophy [12,35]. However, it was unclear whether the up-regulation of MuRF1 and MAFbx differed depending on muscle fiber types in NCI-induced muscle atrophy. In our study, MuRF-1 and MAFbx were up-regulated on day 3 after NCI in both plantaris and soleus muscles. A previous study indicated that the up-regulation of MuRF-1 was induced on day 3 in both fast (plantaris) and slow (soleus) muscles after muscle denervation [35]. Therefore, we speculated that the up-regulation MuRF-1 and MAFbx in an early stage (3rd day) is common in nerve damage-induced atrophy regardless of fiber type.

The expression of myostatin differed between plantaris and soleus muscles. Although previous studies reported that myostatin expression was different according to the muscle fiber type [36-39], whether such difference maintained in NCI-induced atrophy has not been examined. We observed an increased expression of myostatin after NCI only in fast-twitch rich plantaris muscle on day 14 after NCI. Fast-twitch fibers mainly utilize glycolysis for muscle contractions [37]. Because myostatin is related to energy metabolism [40], myostatin-related atrophy is more directed to glycolytic fiber wasting. Moreover, myostatin is expressed mainly in fast twitch fibers and myostatin-induced protein degradation occurs primarily in these fibers [36-39]. Therefore, the expression of myostatin may be enhanced in fast twitch muscles under NCI-induced atrophy.

Although NCI elevated the expression of MuRF-1, MAFbx and myostatin, these changes were not coordinated in a time-dependent manner. An increased expression of myostatin reportedly up-regulates the UPS [23]. This finding is inconsistent with the high expression of ubiquitin proteolytic system that is found to be involved in the myostatin-UPS axis. However, in a previous study, the expression of myostatin in gastrocnemius muscle was found to increase significantly by NCI from 7th day to 14th day [26]. In human study, it was also

reported that the expression of myostatin is later than that of MuRF1 and MAFbx expression [41].

In conclusion, MuRF-1 and MAFbx were up-regulated on day 3 after NCI in both plantaris and soleus muscles, whereas the expression of myostatin significantly increased on day 14 only in plantaris muscle. These results suggest that the expression of myostatin is correlated with atrophy of fast twitch muscle fibers, and is independent of the activation of E3 ubiquitin ligases. Our findings will provide important information into the development of therapies that can be used to prevent skeletal muscle atrophy under specific nerve injuries.

Acknowledgment

This study was supported by graduate school of health and sport sciences of Nippon Sport Science University. The authors would like to thank Nippon Sport Science University for support.

Conflict of Interest

The authors report no conflicts of interest related to this study.

References

1. Jackman RW, Kandarian SC. The molecular basis of skeletal muscle atrophy. Am J Physiol Cell Physiol 2004; 287: C834-843.
2. Phillips SM, Glover EI, Rennie MJ. Alterations of protein turnover underlying disuse atrophy in human skeletal muscle. J ApplPhysiol 2009; 107: 645-654.
3. Vinciguerra M, Musaro A, Rosenthal N. Regulation of muscle atrophy in aging and disease. Adv Exp Med Biol 2010; 694: 211-233.
4. Bodine SC, Baehr LM. Skeletal muscle atrophy and the E3 ubiquitin ligases MuRF1 and MAFbx/atrogin-1. Am J Physiol Endocrinol Metab 2014; 307: 469-484.
5. Bodine SC, Latres E, Baumhueter S, Lai VK, Nunez L, Clarke BA, Poueymirou WT, Panaro FJ, Na E, Dharmarajan K, Pan ZQ,Valenzuela DM, DeChiara TM, Stitt TN, Yancopoulos GD, Glass DJ. Identification of ubiquitin ligases required for skeletal muscle atrophy. Science. 2001; 294: 1704-1708.
6. Wang Y, Pessin JE. Mechanisms for fiber-type specificity of skeletal muscle atrophy. Curr Opin Clin Nutr Metab Care 2013; 16: 243-250.
7. Beehler BC, Sleph PG, Benmassaoud L, Grover GJ. Reduction of skeletal muscle atrophy by a proteasome inhibitor in a rat model of denervation. Exp Biol Med (Maywood) 2006; 231: 335-341.
8. Isfort RJ, Hinkle RT, Jones MB, Wang F, Greis KD, Sun Y, Keough TW, Anderson NL, Sheldon RJ. Proteomic analysis of the atrophying rat soleus muscle following denervation. Electrophoresis 2000; 21: 2228-2234.
9. Isfort RJ, Wang F, Greis KD, Sun Y, Keough TW, Bodine SC, Anderson NL. Proteomic analysis of rat soleus and tibialis anterior muscle following immobilization. J Chromatogr B Analyt Technol Biomed Life Sci 2002; 769: 323-332.
10. Nagatomo F, Fujino H, Kondo H, Suzuki H, Kouzaki M, Takeda I, Ishihara A. PGC-1a and FOXO1 mRNA levels and fiber characteristics of the soleus and plantaris muscles in rats after hindlimb unloading. Histol Histopathol 2011; 26: 1545-1553.
11. Moriscot AS, Baptista IL, Bogomolovas J, Witt C, Hirner S, Granzier H, Labeit S. MuRF1 is a muscle fiber-type II associated factor and together with MuRF2 regulates type-II fiber trophicity and maintenance. J Struct Biol 2010; 170: 344-353.
12. Okamoto T, Torii S, Machida S. Differential gene expression of muscle-specific ubiquitin ligase MAFbx/Atrogin-1 and MuRF1 in response to immobilization-induced atrophy of slow-twitch and fast-twitch muscles. J Physiol Sci 2011; 61: 537-546.
13. Picard M, Ritchie D, Thomas MM. Alterations in intrinsic mitochondrial function with aging are fiber type-specific and do not explain differential atrophy between muscles. Aging Cell 2011; 10: 1047-1055.
14. Wu P, Chawla A, Spinner RJ, Yu C, Yaszemski MJ, Windebank AJ, Wang H. Key changes in denervated muscles and their impact on regeneration and reinnervation. Neural Regen Res 2014; 9: 1796-1809.
15. Goodman CA, Mayhew DL, Hornberger TA. Recent progress toward understanding the molecular mechanisms that regulate skeletal muscle mass. Cell Signal 2011; 23: 1896-1906.
16. Ciciliot S, Rossi AC, Dyar KA, Blaauw B, Schiaffino S. Muscle type and fiber type specificity in muscle wasting. Int J Biochem Cell Biol 2013; 45: 2191-2199.
17. De Palma L, Marinelli M, Pavan M, Orazi A. Ubiquitin ligases MuRF1 and MAFbx in human skeletal muscle atrophy. Joint Bone Spine Revue du Rhumatisme 2008; 75: 53-57.
18. Kimura N, Kumamoto T, Oniki T, Nomura M, Nakamura K, Abe Y, Hazama Y, Ueyama H. Role of ubiquitin-proteasome proteolysis in muscle fiber destruction in experimental chloroquine-induced myopathy. Muscle Nerve 2009; 39: 521-528.
19. Clavel S, Coldefy AS, Kurkdjian E, Salles J, Margaritis I, Derijard B. Atrophy-related ubiquitin ligases, atrogin1 and MuRF1 are up-regulated in aged rat Tibialis Anterior muscle. Mech Age Develop 2006; 127: 794-801.
20. Edstrom E, Altun M, Hagglund M, Ulfhake B. Atrogin-1/MAFbx and MuRF1 are downregulated in aging-related loss of skeletal muscle. J Gerontol Series A Biol Sci Med Sci 2006; 61: 663-674.
21. Labeit S, Kohl CH, Witt CC, Labeit D, Jung J, Granzier H. Modulation of muscle atrophy, fatigue and MLC phosphorylation by MuRF1 as indicated by hindlimb suspension studies on MuRF1-KO mice. J Biomed Biotechnol 2010; 2010: 693-741.
22. Rodriguez J, Vernus B, Chelh I, Cassar-Malek I, Gabillard JC, Hadj Sassi A, Seiliez I, Picard B, Bonnieu A.

Myostatin and the skeletal muscle atrophy and hypertrophy signaling pathways. Cell Mol Life Sci 2014; 71: 4361-4371.

23. McFarlane C, Plummer E, Thomas M, Hennebry A, Ashby M, Ling N, Smith H, Sharma M, Kambadur R. Myostatin induces cachexia by activating the ubiquitin proteolytic system through an NF-kappaB-independent, FoxO1-dependent mechanism. J Cell Physiol 2006; 209: 501-514.
24. Sandri M, Sandri C, Gilbert A, Skurk C, Calabria E, Picard A, Walsh K, Schiaffino S, Lecker SH, Goldberg AL. Foxo transcription factors induce the atrophy-related ubiquitin ligase atrogin-1 and cause skeletal muscle atrophy. Cell 2004; 117: 399-412.
25. Lokireddy S, McFarlane C, Ge X, Zhang H, Sze SK, Sharma M, Kambadur R. Myostatin induces degradation of sarcomeric proteins through a Smad3 signaling mechanism during skeletal muscle wasting. Mol Endocrinol 2011; 25: 1936-1949.
26. Liu M, Zhang D, Shao C, Liu J, Ding F, Gu X. Expression pattern of myostatin in gastrocnemius muscle of rats after sciatic nerve crush injury. Muscle Nerve 2007; 35: 649-656.
27. Baumann AP, Ibebunjo C, Grasser WA, Paralkar VM.Myostatin expression in age and denervation-induced skeletal muscle atrophy. J Musculoskelet Neuronal Interact 2003; 3: 8-16.
28. Shao C, Liu M, Wu X, Ding F. Time-dependent expression of myostatin RNA transcript and protein in gastrocnemius muscle of mice after sciatic nerve resection. Microsurgery 2007; 27: 487-493.
29. Bertaggia E, Coletto L, Sandri M. Posttranslational modifications control FoxO3 activity during denervation. Am J Physiol Cell Physiol 2012; 302: 587-596.
30. Fjallstrom AK, Evertsson K, Norrby M, Tågerud S. Forkhead box O1 and muscle RING finger 1 protein expression in atrophic and hypertrophic denervated mouse skeletal muscle. J Mol Signal 2014; 9: 9.
31. Seddon HJ. A classification of nerve injuries. Br Med J 1942; 2: 237-239.
32. Staron RS, Kraemer WJ, Hikida RS, Fry AC, Murray JD, Campos GE. Fiber type composition of four hindlimb muscles of adult Fisher 344 rats. Histochem Cell Biol 1999; 111: 117-123.
33. Higashino K, Matsuura T, Suganuma K, Yukata K, Nishisho T, Yasui N.Early changes in muscle atrophy and muscle fiber type conversion after spinal cord transection and peripheral nerve transection in rats. J Neuroeng Rehabil 2013; 46: 1186-1743.
34. Huey KA, Bodine SC. Changes in myosin mRNA and protein expression in denervated rat soleus and tibialis anterior. Eur J Biochem 1998; 256: 45-50.
35. Gomes AV, Waddell DS, Siu R, Stein M, Dewey S, Furlow JD, Bodine SC. Upregulation of proteasome activity in muscle RING finger 1-null mice following denervation. FASEB J Publ Feder Am Soc Exp Biol 2012; 26: 2986-2999.
36. Girgenrath S, Song K, Whittemore LA. Loss of myostatin expression alters fiber-type distribution and expression of myosin heavy chain isoforms in slow- and fast-type skeletal muscle. Muscle Nerve 2005; 31: 34-40.
37. Mendias CL, Marcin JE, Calerdon DR, Faulkner JA. Contractile properties of EDL and soleus muscles of myostatin-deficient mice. J Appl Physiol 2006; 101: 898-905.
38. Hennebry A, Berry C, Siriett V, OCallaghan P, Chau L, Watson T, Sharma M, Kambadur R. Myostatin regulates fiber-type composition of skeletal muscle by regulating MEF2 and MyoD gene expression. Am J Physiol Cell Physiol 2009; 296: 525-534.
39. Macpherson PC, Wang X, Goldman D. Myogenin regulates denervation-dependent muscle atrophy in mouse soleus muscle. J Cell Biochem 2011; 112: 2149-2159.
40. Mouisel E, Relizani K, Mille-Hamard L, Denis R, Hourdé C, Agbulut O, Patel K, Arandel L, Morales-Gonzalez S, Vignaud A, Garcia L, Ferry A, Luquet S, Billat V, Ventura-Clapier R, Schuelke M, Amthor H. Myostatin is a key mediator between energy metabolism and endurance capacity of skeletal muscle. Am J Physiol Regul Integr Comp Physiol 2014; 307: 444-454.
41. Louis E, Raue U, Yang Y, Jemiolo B, Trappe S. Time course of proteolytic, cytokine, and myostatin gene expression after acute exercise in human skeletal muscle. J Appl Physiol (1985) 2007; 103: 1744-1751.

*Correspondence to

Hongsun Song

Department of Sports Science

Korea Institute of Sport Science

Seoul

Korea